THE MODIFICATION OF SPIRAL CASE AND IMPELLER OF MIXED FLOW PUMP

Roman Klas*, František Pochylý*

This paper is aimed at differences in designs of spiral case and impeller of mixed flow pump with regard to suppression of Y-Q characteristic curves instability, pressure pulsations and especially to achieving necessary delivery head. The differences between new and old conception will be explained. The reasons of these differences with regard to flow in pump interior, hydraulic losses, static pressures and velocities will be explained as well.

Keywords: *impeller, spiral case, Y-Q characteristic curve, instability, discharge*

1. Introduction

To make a good proposal of any hydrodynamic pump is not an easy task. The ways how to achieve it are usually well protected know-how of every specialist department. However, in many cases it is possible to use only basic relations and laws that are able to define the scope and possibilities for another new proposal. Some problems that can be connected with operation of hydraulic machine can be also avoided this way. To the most important parameters belong the delivery head, the stability of Y-Q characteristic curves and related undesirable pressure pulsations.

Two radiaxial pumps with the same design parameters will be used to demonstrate the above mentioned possibilities. First the disadvantages will be outlined and second possible solutions will be shown and demonstrated. Pump operation will be simulated by means of CFD software. Measured characteristic curve is at disposal for the problematic pump.

2. Nomenclature

Mark	Title	Unit
1	inlet	
2	outlet	
c_u	circumferential component of absolute velocity	$[\mathrm{m\,s^{-1}}]$
D_2	impeller diameter	[m]
Q	mass flowrate	$[\mathrm{kg\,s^{-1}}]$
Q_v	volume flowrate	$[\mathrm{m^3 s^{-1}}]$
S	area	$[\mathrm{m^2}]$
u	circumferential component of velocity	$[\mathrm{m\,s^{-1}}]$
v	absolute velocity	$[\mathrm{m\,s^{-1}}]$
Y	specific energy	$[\mathrm{J\,kg^{-1}}]$

* Ing. R. Klas, Ph.D., prof. Ing. F. Pochylý, CSc., Technical University of Brno, Faculty of Mechanical Engineering, Victor Kaplan Department of Fluids Engineering, Technická 2, 616 69, Brno, CR

Y_t	theoretical specific energy	$[J\,kg^{-1}]$
Δp	difference of static pressures	[Pa]
β	blade angle	[°]
φ	circumferential wrap angle	[°]
ν	kinematic viscosity	$[m^2s^{-1}]$

3. Numerical simulation and calculation conditions

The models of both hydraulic designs were created in preprocessor GAMBIT 2.4.6 and consisted of complete impeller and spiral case. The gaps between shroud and spiral case and between hub and pump casing will be omitted only. The former will be referenced as Pump 1, the latte one as Pump 2. Further will be mentioned as Pump 1 and Pump 2 (Fig. 1). More detailed information can be found in Tab. 1.

The impeller of PUMP 1 has four blades and the impeller of PUMP 2 consists of five blades. Subsequent numerical simulation in range of Y-Q characteristic curve was performed in software Ansys Fluent 12.1. The basic calculation parameters are summarized in Tab. 2.

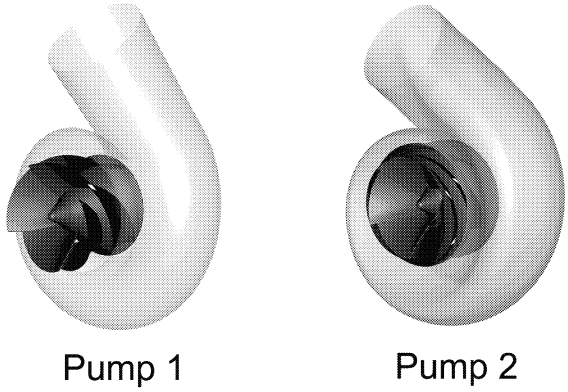

Fig.1: The insight into PUMP 1 and PUMP 2 geometry

	PUMP 1	PUMP 2
Average value of blade angle β_2	24.7	21.5
Impeller diameter D_2	0.296	0.315
Reynolds number $Re = u_2\,D_2/\nu$	8765968	9927447

Tab.1: Basic pump parameters

Number of computational cells	8.5 millions
Turbulence model	k-εrealizable non equilibrium wall function
Calculation mode	unsteady sliding mesh incompressible flow
Boundary conditions	Inlet: velocity inlet Outlet: pressure outlet

Tab.2: Basic calculation parameters

4. Specific energy

The required value of specific energy for defined flow rate is definitely the basic parameter of every pump. Its value in design point can be set from Euler pump equation (1), that is completed with hydraulic efficiency and correction for final blade number, i.e. correction for slip factor. We use only the equation for theoretical value of specific energy in this case. The basic design for PUMP 2 design was made by singularity method and subsequently was corrected by CFD simulation in Fluent software. So the slip factor was not used.

$$Y_\mathrm{t} = u_2\, c_{\mathrm{u}2} - u_1\, c_{\mathrm{u}1}\ . \tag{1}$$

If we express the respective equation as the dependence on flow rate (2), we can plot the value of theoretical specific energy into a graph and then limit the boundaries in which we can move with our design.

$$Y_\mathrm{t} = u_2 \left(u_2 - \frac{Q_\mathrm{v}}{S_2\, \tan\beta_2} \right) - u_1 \left(u_1 - \frac{Q_\mathrm{v}}{S_1\, \tan\beta_1} \right)\ . \tag{2}$$

To plot it we use the data for PUMP 1 (Fig. 2) and for PUMP 2 (Fig. 3). It is well known that the value of term $u_1\, c_{\mathrm{u}1}$ is zero in range of flow rates of $0.75\, Q_\mathrm{BEP}$ and $1.25\, Q_\mathrm{BEP}$. Further trend of $u_1\, c_{\mathrm{u}1}$ corresponds to equation (2). The curves of specific energy obtained from CFD calculations will be drawn here as well as the theoretical curves. Furthermore the measured curve of actual specific energy of real pump will be shown for PUMP 1.

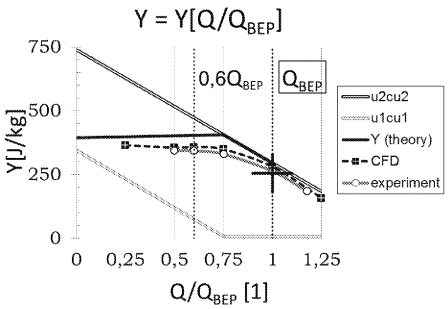

Fig.2: Theoretical Y-Q characteristic curve, measured data for PUMP 1

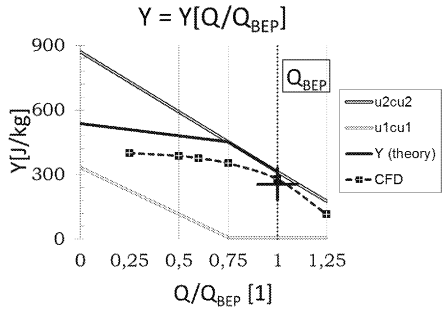

Fig.3: Theoretical Y-Q characteristic curve, measured data for PUMP 2

The design parameters are marked by the cross in the graph. The realized experiment was carried out in company Sigma and there are no detailed records about its course with respect to the date of realization. Particularly we can observe that in case of Fig. 2 the theoretical curve for specific energy is virtually parallel with axis of mass flow rate. The actual value of delivery head is nevertheless smaller because of losses. In order to achieve the stability of curve for delivery head in dependency of flow rate it is necessary that the losses increase with the increasing flow rates. However, in the spiral case the losses increase on the right as well as on the left from best efficiency point.

So, it is appropriate for the theoretical value of specific energy to have sufficiently steep curve. Then there will be a chance for stable curve of specific energy also after including the losses in impeller and spiral case (Fig. 3). Evidently the value of quadratic terms for peripheral velocities u_1^2 and u_2^2 (for infinite number of very thin blades) is related to design of impeller. Its shape is limited by the value of specific speed and consequently by impeller operation. Therefore these values cannot be changed at will.

5. Influence of spiral case and impeller on Y-Q characteristic curve

Two main methods used for spiral case design are defined by simple equations $c_u R =$ $=$ const. and $c_u S =$ const. Both are sufficiently described in literature [1], [2] and both lead to approximately linear increase of flow spiral case area with its developed length. The shapes of individual flow areas as well as placing the nose of spiral case are obviously fundamental. The dependency of cross-sectional area on spiral case angle measured in circumferential direction for both pumps can be seen on Fig. 4.

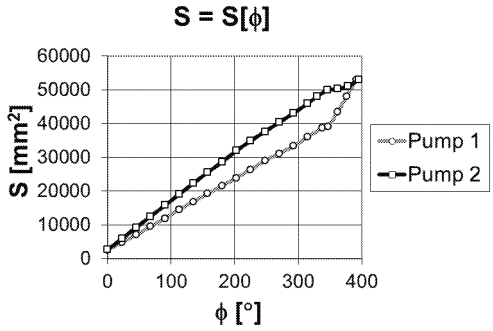

Fig.4: Variation of areas in spiral case of PUMP 1 and PUMP 2

We can say, in respect to spiral case design, that the position of blade trailing edges corresponds to radiaxial pump layout, whereas the hub and shroud have the same outlet diameter Fig. 5. The spiral case is also more open and cross-sectional area increase more steeply. Sections after break of curves correspond to the diffuser. For PUMP 1 it is obvious, that rising of flow area in diffuser is extreme.

The results of it can be seen in Fig. 6 describing the change of static pressure difference in spiral case with flow rate.

This figure indicates that PUMP 1 reaches the higher pressure difference in spiral case, but it happens in region of relatively high flow rates. Then in combination with practically linear change of static pressure in impeller (Fig. 7) it can cause the formation of inflexion for sum of pressure differences of impeller and spiral case (Fig. 8). Consequently this inflexion

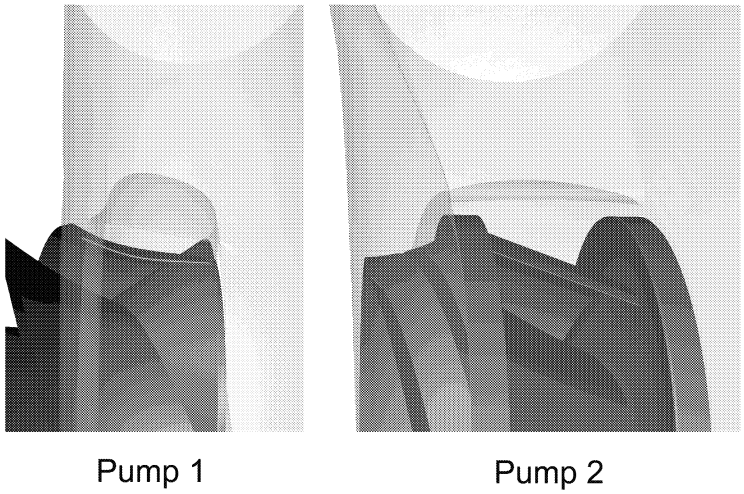

Fig.5: Shape of impeller and spiral case nose of PUMP 1 and PUMP 2

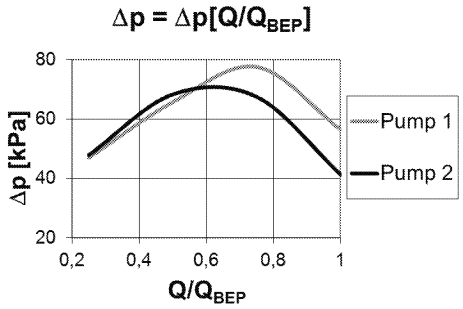

Fig.6: Static pressure difference in spiral case of PUMP 1 and PUMP 2

can also influence the Y-Q characteristic curve and may mean the practically constant value of specific energy in certain range. But the energy after subtraction of the losses definitely remains conserved. Therefore the change is useful with respect to stability, if the drop of losses occurs in corresponding range of flow rates. In Fig. 2 measured characteristic of specific energy ends approximately at value $0.5\,Q_{\mathrm{BEP}}$. It is because of the considerable pressure pulsations, which did not allow further realiable measurement.

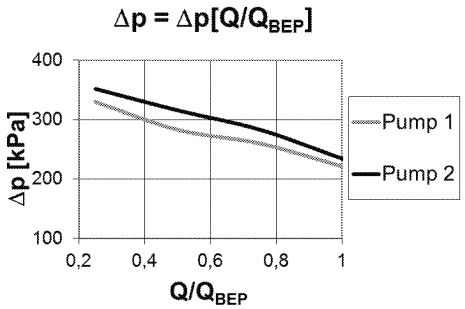

Fig.7: Static pressure difference in impeller of PUMP 1 and PUMP 2

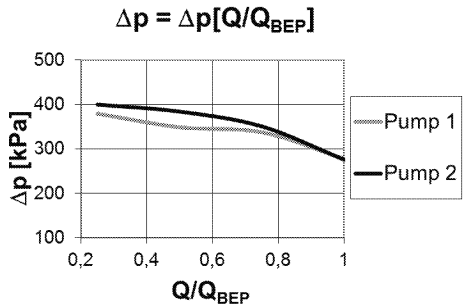

Fig.8: Static pressure difference in impeller and spiral case of PUMP 1 and PUMP 2

Although the spiral case of PUMP 2 achieves the lower pressure differences in Fig. 6, the maximum of this function lies near $0.6\,Q_{\mathrm{BEP}}$. The curve of this function is also a bit flatter than for PUMP 1. Therefore it is indicated, that it might be profitable to try to achieve the necessary value of static pressure (specific energy) mostly by means of impeller and not by spiral case. This has also the positive influence on stability of Y-Q characteristic curve [3]. This of course corresponds with Fig. 4. In this connection it will be interesting to view the theoretical trend of mean velocities in individual cuts through the spiral case Fig. 9.

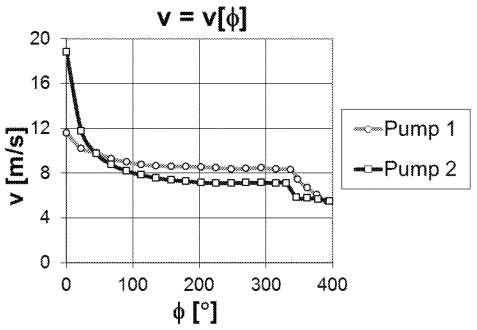

Fig.9: Theoretical velocities course in spiral case

Two curves are displayed here. First curve corresponds to trend of theoretical velocities in spiral case of PUMP 1, second curve in spiral case of PUMP 2. The velocities agree with linear increase of mass flow rate along the spiral case perimeter and so every blade channel supplies the spiral case equally. However we will focus on the mass flow rate under the spiral case nose corresponding to the best efficiency point.

Theoretical trend of mean velocities in spiral casing cuts indicates that the velocity downstream the spiral case nose decreases in best efficiency point. Subsequently it maintains on practically constant value and then decreases in diffuser. In compliance with energy conservation the distribution of static pressure corresponds to this. (Naturally it is also necessary to respect the influence of losses.)

Now we can check how the real values of mass flow rates develop in individual spiral case cuts for individual operating point. Fig. 10 provides the view of mass flow rates in range $0.25\,Q_{\mathrm{BEP}}-1.25\,Q_{\mathrm{BEP}}$ for PUMP 1. It is obvious, that the mass flow rate curves sharply bow approximately on level 70° downstream the spiral case nose. This is indicated also by two straight lines marked as 0.75 and 1.25, which represent the values Q/Q_{BEP}. The curves

of flow rates $0.75\,Q_{\mathrm{BEP}}$ and $1.25\,Q_{\mathrm{BEP}}$ correspond to these values. The curve of flow rate $0.75\,Q_{\mathrm{BEP}}$ is remarkable. This curve lies near the spiral case nose above the curve of best efficiency flow rate. Analogical Fig. 11 was made for PUMP 2.

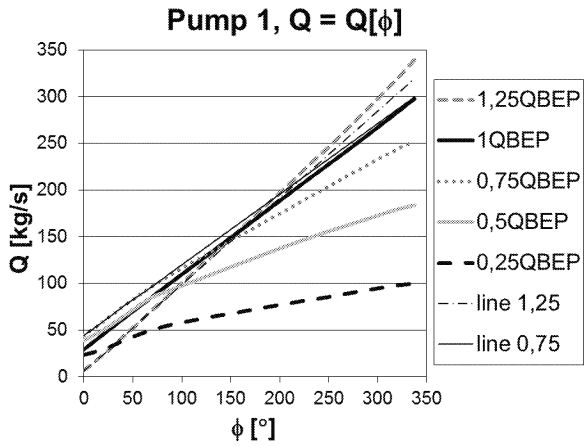

Fig.10: Mass flow rates in spiral case in individual cuts, PUMP 1

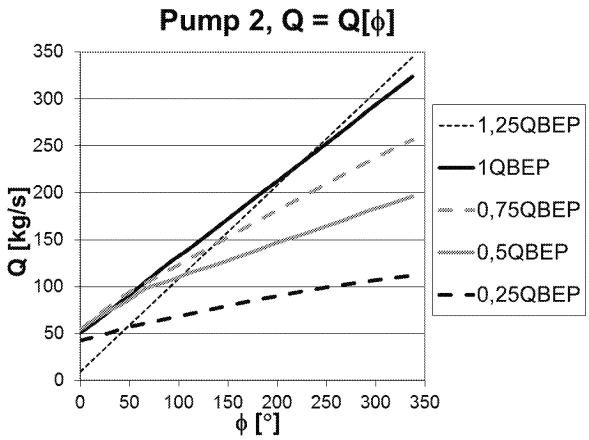

Fig.11: Mass flow rates in spiral case in individual cuts, PUMP 2

If we plot the values of flow rates for PUMP 1 (Fig. 12) and PUMP 2 (Fig. 13) in individual cuts along the spiral case perimeter and for individual operating point, we can observe considerably nonlinear trend of drawn curves. All these curves belong to PUMP 1. Theoretically it can be assumed of course that the mass flow rate in cuts will increase together with linearly increasing pump mass flow rate. However, the breakpoint can be found lying between $0.6\,Q_{\mathrm{BEP}}$ and $0.8\,Q_{\mathrm{BEP}}$ for PUMP 1 and its spiral case. Mass flow rates in all cuts steeply decrease from this point towards the lower mass flow rates. Also towards the higher operating flow rates the amount of flowing liquid decreases in approximately half of cuts. The breakpoint lying in flow rate interval $0.4\,Q_{\mathrm{BEP}}$ and $0.6\,Q_{\mathrm{BEP}}$ can be observed in case of PUMP 2 Fig. 13. Nevertheless the difference lies in fact, that the mass flow rate in remaining cuts is either constant or increasing towards the spiral case outlet.

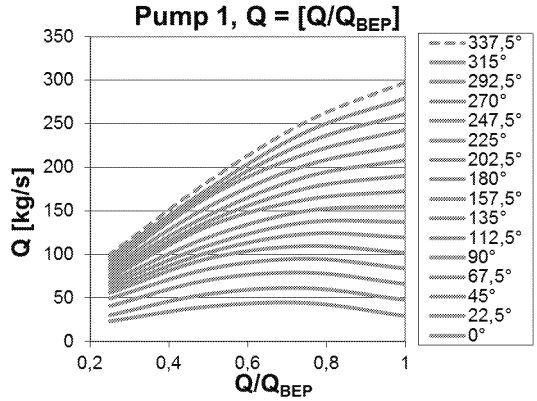

Fig.12: Mass flow rates in spiral case in individual cuts and operating points

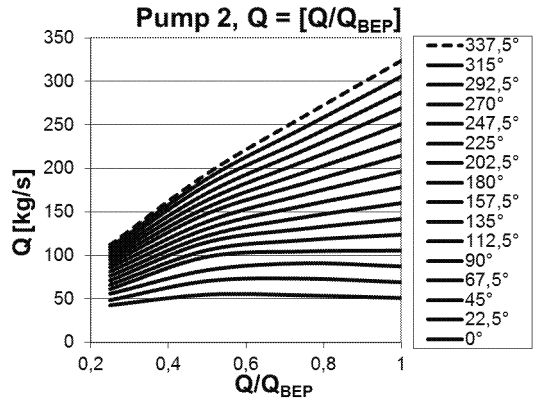

Fig.13: Mass flow rates in spiral case in individual cuts and operating points

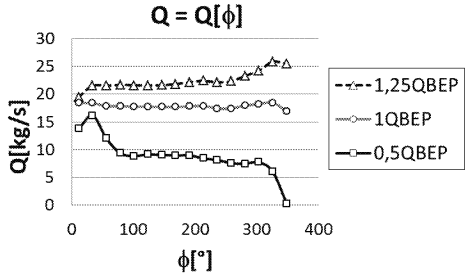

Fig.14: Mass flow rates delivered by PUMP 1 into spiral case

This comparison provides the differences that result from the different concept of spiral case nose (see Fig. 5) as well as areas (see Fig. 4). Whereas the cross-section below the spiral case nose is almost the same for both pumps. But the concept of PUMP 1 causes the massive spatial swirling downstream the spiral case nose that changes its orientations with decreasing flow rate. In case of PUMP 2 the flow in this area is more uniform with regards to axis of symmetry.

Respecting the mass flow rates, that are supplied by blade channels to spiral case (Fig. 14 – PUMP 1), it is possible to say that the spiral case is filled in principle equally by impeller

in best efficiency point. Stable value of mass flow rate on these curves changes linearly with increasing amount of delivered liquid. Analogous results would be obtained also for PUMP 2.

6. Conclusions

As was it stated at the beginning of this paper, it is important to respect the basic equations describing the energy transformation in hydrodynamic machines during design of every pump. These equations can define basic scope that limits the theoretical possibilities of these machines. Euler pump equation for infinite number of very thin blades including the circulation of liquid upstream the impeller is able to fulfil exactly this function. And so it can predict the curve of specific energy including its stability. Here it is necessary to point out, that especially in point with zero mass flow rate $Q = 0$ (shut-off point) it is needed to consider the influence of finite number of blades as well. Therefore for another analysis it is necessary to turn to specialized literature. But with respect to fact, that theoretical specific energy value for finite number of blades (without considering the hydraulic efficiency) will be lower in point $Q = 0$, then the situation can be even more critical. However it is possible to rely on zero value of liquid circulation upstream the impeller in range $0.75\,Q_{\mathrm{BEP}}-1.25\,Q_{\mathrm{BEP}}$.

Situation from the point of the spiral case cross-sections looks better for PUMP 2, which predicts the dependency of specific energy on flow rates obtained by means of CFD. It should also be mentioned, that the PUMP 2 has more blades and therefore it is possible to put greater reliance on Euler pump equation as is written in (1).

Besides the parameter describing the energy transformation in impeller it is essential to discuss also the role of spiral case. In spiral case of PUMP 1 the diffusion occurs predominantly in outlet neck. It is comprehensible that in classic conic diffuser the change of kinetic energy into pressure cannot occur with the same increment of pressure in range of mass flow rate $(0-1)\,Q_{\mathrm{BEP}}$. The diffusion does not occur only in the neck, the whole spiral case contributes to this process. With respect to length of spiral case circumference (measured e.g. on the side of impeller) it is obvious, that its length is bigger than distance between last spiral case cut and outlet of spiral casing (i.e. length of spiral case neck). Therefore the change of kinetic energy into pressure can occur more gradually. On the other hand too much open spiral case can imply risk of undesirable vortex generation and resulting losses.

It is well known, that with respect to the design of spiral casing the spiral case nose as well as sector downstream this spiral case nose is very important. The sector can be defined approximately on 70° – measured from spiral case nose. Therefore it is apparent, that for PUMP 1 the restriction of discharge occurs exactly in this sector. Besides the insufficient size of flow area the reason consists in the angle, under which the liquid leaves the impeller and approaches the spiral case nose. Naturally the spiral case is designed for the best efficiency point, but in others regimes of pump operation the flow separation can occur from spiral case nose on the side of impeller or spiral case neck. This fact can be proved by velocity field pattern in place of spiral case nose with respect to different size of liquid meridional velocity. The liquid circulation in spiral case is higher for PUMP 2. This reflects filling of spiral case around the spiral case nose as well as in other spiral case cuts for low or high flow rates. This fact is illustrated also by static pressure difference in spiral case in PUMP 2. As was stated, diffusion in PUMP 2 occurs predominantly through spiral case itself, which consequently assists to extending the area, where the kinetic energy of liquid changes into

pressure energy. This is worthless without the shift towards low discharges, where eventual instability is assumed. This idea is supported by location of pressure difference maximum.

However, above mentioned facts will be also dependent on parameters of given hydrodynamic machine and it is essential to consider them in context of particular specific speed.

Acknowledgement

This work was supported by the grant project FSI-S-12-2 and also by the project CZ.1.07/2.3.00/30.0005.

References

[1] Paciga A., Strýček O., Gančo M.: Čerpacia technika, Alfa 1984, Bratislava, p. 92–98
[2] Stepanoff A. J.: Centrifugal and axil flow pumps, 2nd edition, John Willey&Sons 1957, New York, p. 110–123
[3] Pochylý F., Haluza M., Klas R.: Earth Environ. Sci., 12, 2010, p. 685

Received in editor's office: November 6, 2012
Approved for publishing: April 12, 2013